**International Journal of Power Electronics and Drive Systems (IJPEDS)**
Vol. 12, No. 3, September 2021, pp. 1813~1822
ISSN: 2088-8694, DOI: 10.11591/ijpeds.v12.i3.pp1813-1822 

# Comparison of PV panels MPPT techniques applied to solar water pumping system

**Islam K. Abdul-Razzaq[1], Mohamed M. Fahim Sakr[2], Yasir G. Rashid[3]**
[1,2]Department of Electrical Power Engineering, College of Engineering, Cairo University, Giza, Egypt
[3]Department of Electronic Engineering, College of Engineering, Diyala University, Diyala, Iraq

**Article Info**

***Article history:***

Received Apr 13, 2021
Revised Jul 1, 2021
Accepted Jul 12, 2021

***Keywords:***

Fractional open voltage circuit
Fractional short current circuit
Incremental conductance
Perturb and observe
Solar water pumping system
Maximum power point trackers

**ABSTRACT**

This paper deals with an advanced design for a pump powered by solar energyto supply agricultural lands with water and also the maximum power point is used to extract the maximum value of the energy available inside the solar panels and comparing between techniques MPPT such as Incremental conductance, perturb & observe, fractional short current circuit, and fractional open voltage circuit to find the best technique among these. The solar system is designed with main parts: photovoltaic (PV) panel, direct current/direct current (DC/DC) converter, inverter, filter, and in addition, the battery is used to save energy in the event that there is an increased demand for energy and not to provide solar radiation, as well as saving energy in the case of generation more than demand. This work was done using the matrix laboratory (MATLAB) simulink program.



***Corresponding Author:***

Yasir G. Rashid
Department of Electronic Engineering
College of Engineering, University of Diyala
Baqubah, 32001 Diyala, Iraq
Email: yasserghazee_enge@uodiyala.edu.iq

## 1. INTRODUCTION

Solar energy is one of the available renewable energy resources that can provide us with steady, reliable power [1]. However, because sunlight does not need any kind of fuel, solar energy can be used directly to create electricity. No gases or poisons are emitted into the air. Solar power systems need minimal maintenance. Solar modules have a service life of 25 years without lubrication or maintenance. Using solar energy does have one drawback, however: It is expensive. As long as the sun doesn't shine for 24 hours a day, the solution involves the combination of a photovoltaic system and a battery. It is useful in nearly any place, particularly if there is sunlight and access to clean water. When a user of a solar water application opens a faucet, water is applied to the tank from above [2]-[4]. Figure 1 depicts the daily supply of solar water.

PV systems frameworks are being used more to increase their energy-efficiency by using PV systems. But due to the low module efficiency, there is still a device capacity problem in photovoltaic systems [4]. As a result, matching the maximum electrical output to a photovoltaic device requires careful evaluation of its constituents. Placing only requires choosing the best PV modules and implementing an efficien maximum power point tracking (MPPT) algorithm.

In literature, a multitude of MPPT schemes for solar PV systems have been presented in books and journal articles. Many techniques vary in difficulty, hardware, popularity, and availability, among other variables. An approach which has found broad acceptance in PV tracking is based on this technique, but not limited to, perturbation & observation (P&O) (which is the most known), the incremental conductance (INC),

fractional short current circuit and fractional open voltage circuit [5]-[7]. In this work, the emphasis will be on design and simulation of solar water pumping systems and comparison study between widely applied MPPT techniques, while considering weather conditions will be on assessing which method is the most capable of shifting resource patterns in short order.

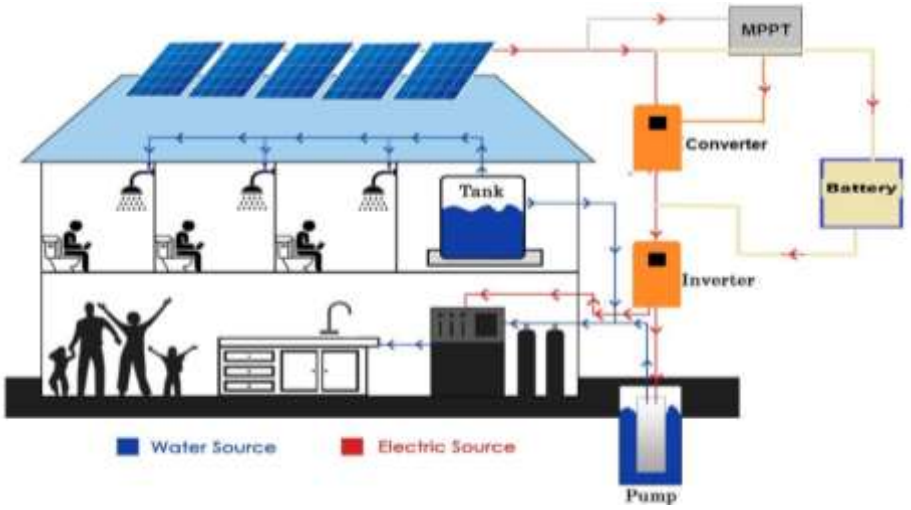


Figure 1. Solar water daily supply

## 2. PHOTOVOLTAIC SYSTEM MODELLING

Figure 2 shows the main block diagram of the proposed stand-alone system. The first block is represented by photovoltaic solar panels. The voltage and current that gets sent to the output of the MPPT controller will be measured by a sensing circuit. A boost converter DC/DC power electronic switch uses pulse width modulation (PWM) to vary its duty cycle. The battery is still charged, which means the rest of the blocks are represented by PWM. The inverter output voltage will be sensed by sensing circuit that to be used for modulation index control to stabilize the inverter alternating current (AC) voltage level [8], [9].

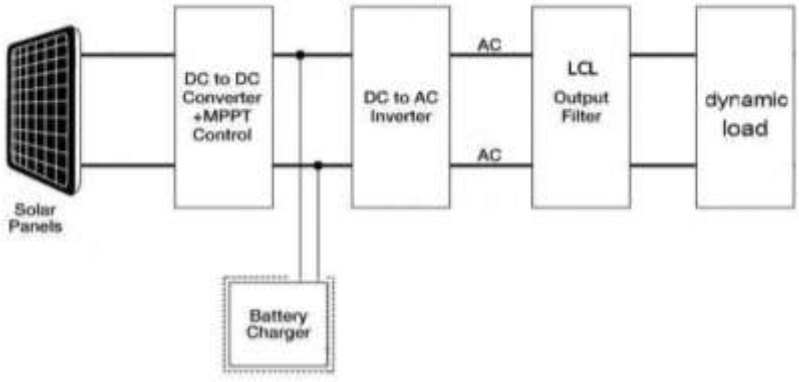


Figures 2. The stand-alone PV system block diagram

### 2.1. Photovoltaic generator model

When there is low electricity production from PV cells. As a result, the cells should be laid out in a parallel-serial fashion, where the energy is created in several modules. A photovoltaic panel is composed of series and parallel modules. The PV panel design begins with selecting CS6P-250P solar cell type Monocrystalline Maxeon Gen II PV modules. Table 1 also includes a summary of the spectifications of the PV panel parameters. PV panels will be used in this project, which will include 80 panels (total capacity is 20 Kw). These panels are organized into eight parallel lines, each of which contains ten serially linked panels

[10]. Figure 3 shows solar cellsequivalent circuit in $N_s$ -series and $N_p$ -parallel is shown in and the formula for their $V_T$ and $I_T$ [11], [12]:

$$I_T = N_P . I_{Ph} - N_P . I_o \left[\exp\left(\frac{V_T}{N_s.k_o} + \frac{I_{sa}.R_s}{N_p.k_o}\right) - 1\right] - \frac{1}{R_p}\left(\frac{V_T}{N_s} + \frac{I_{sa}.R_s}{N_p.k_o}\right) \quad (1)$$

where $k_o = \mathrm{AKT/q}$ , $I_{Ph}$ is light-generated current; $I_{sa}$ cell reverse saturation current; A is ideality factor (=1); T is cell temperature (in Celsius); K is Boltzmann's constant (= 1.3805 × $10^{-23}$ N m/K); q is electronic charge (=1.6×$10^{-19}$ C); $R_s$ and $R_p$ is the series and parallel resistance respectively, $N_P . I_{Ph}$ is the solar short-circuit current. To learn more about the differences in the impact of different irradiation levels on the P-V and I-V characteristics, see Figure 4 and Figure 5.

Table 1. Spicefications of CS6P-250 MPV model [13]

| Property | Value |
|---|---|
| Maximum Power (Pmax) (W) | 250 W |
| Voltage at Pmax (V) | 30.4 V |
| Current at Pmax (A) | 8.22 A |
| Open-circuit voltage (Voc) (V) | 37.5 V |
| Short-circuit current (Isc) (A) | 8.74 A |
| Temperature coefficient of Power (%/K) | -0.45 |
| Temperature coefficient of Voc (%/K) | -0.35 |
| Temperature coefficient of iSC (%/K) | -0.06 |
| Cell type (e) | Monocrystalline |
| Module efficiency | 15.54% |
| Dimensions (mm) | 1638 (h) x 982 (w) 40 (d) |
| Weight | 20 kg |

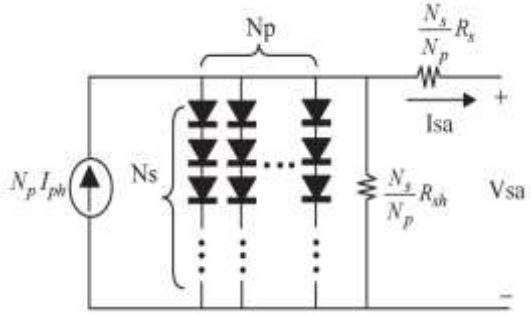


Figure 3. Solar panel electrically equivalent circuit [12]

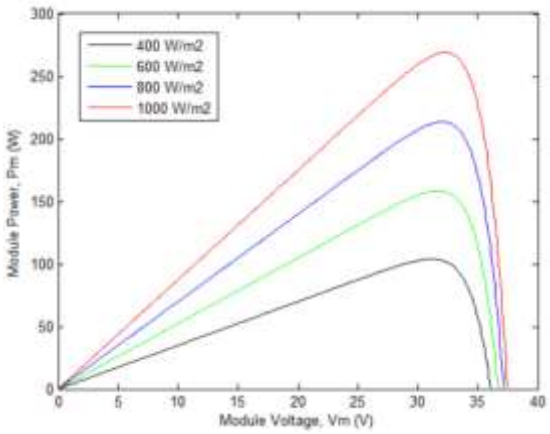


Figure 4. At T=25 °C, the P-V characteristics for various solar irradiance (G) values are shown

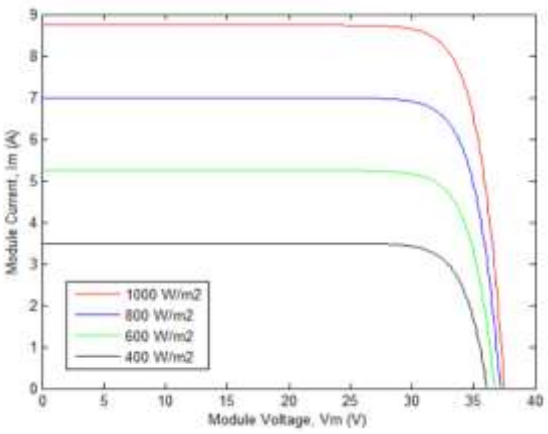


Figure 5. At T=25 °C, the I-V characteristics for various solar irradiance (G) values are shown

### 2.2. Boost converter model

By interposing a power converter (DC-DC converter) between the photovoltaic generator and the load (battery), the MPPT can be achieved. By acting on the converter duty cycle (D), the operation point can be guaranteed to be the MPPT. It uses step-up methodology. The voltage the sensor produces is larger than the voltage that is fed into it. The circuit shown in Figure 6 has an inductor, a capacitor, a switch, and a diode [14]. When the switch is closed, the diode tends to be reverse biased and the current increases through the inductor. When the switch is switched off, the diode tends to be forward biased, the inductive voltage stored in the capacitor is discharged, and the current is allowed to flow through the inductance. Once the voltage has been increased, it is routed to the load. The duty cycle is calculated using the values of the input and output voltages specified in the (2).

$$V_{out} = \frac{V_{in}}{1-D} \quad (2)$$

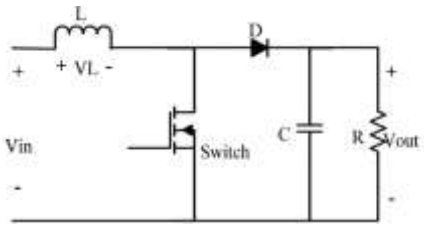


Figure 6. The boost converter circuit

### 2.3. MPPT techniques

The MPPT control is a key component of the PV system. It is critical to optimal system operation. This control approach is derived from the principle of optimal variation of the cyclic ratio D, and we will present and explain later the most popular control techniques. There are a number of common and practical models for estimating how much a PV power will increase with altitude, including perturb & observe, incremental conductance, and fractional short current circuit and fractional open voltage circuit [15], [16].

#### 2.3.1. Perturb and observe (P&O) technique

This technique is widely used for tracking the maximum power due to its simple design. This method adjusts the PV module voltage and compares the new power output with that of the previous perturbation cycle in order to see if it has returned to normal. On the same principle as shown in Figure 7, the PV module voltage shifts the control system in this direction if the PV output voltage rises, and the power is limited if it doesn't [17], [18].

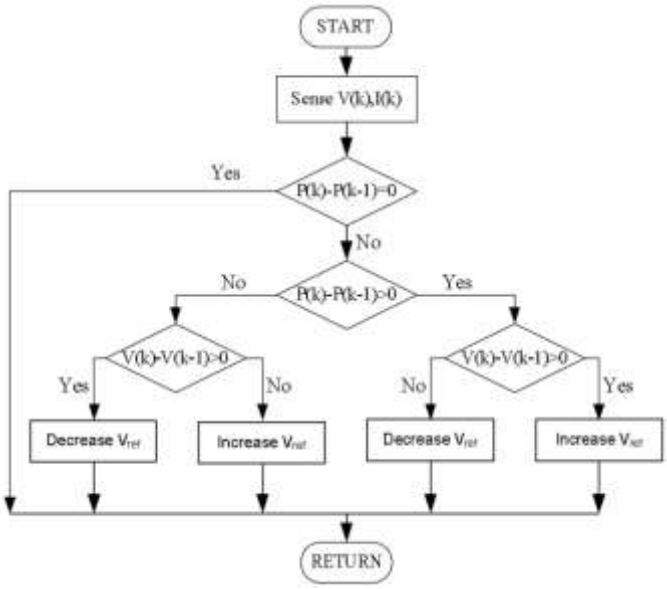


Figure 7. The flowchart of the P&O technique

#### 2.3.2. Incremental conductance (IC) MPPT technique

Incremental conductance technique employs an array terminal voltage that is based on the MPPT voltage. Here is the diagram for this technique in Figure 8. The general form of this technique is this [19], [20].

$$\frac{dP}{dV} > 0 \text{ at MPPT} \quad (3)$$

$\frac{dP}{dV} > 0$ at the left of MPPT (4)

$\frac{dP}{dV} > 0$ at the right of MPPT (5)

$\frac{dP}{dV} = \frac{d(VI)}{d(V)} = I + V\frac{dI}{dV}$ (6)

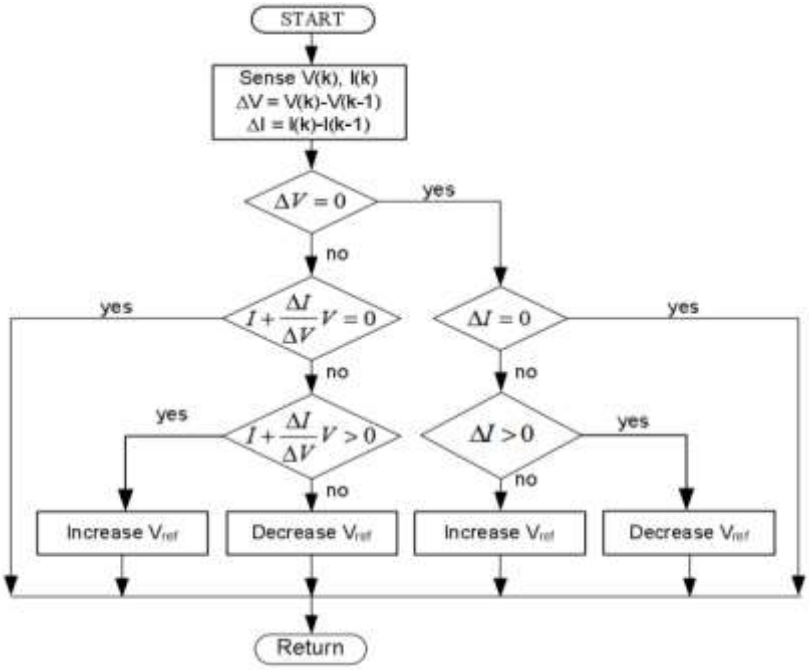


Figure 8. The flowchart of the INC technique

The dP/dV is defined as the identifier factor for the MPPT. The INC technique is proposed to effectively track the MPPT of a photovoltaic panel by utilizing this factor. The definitions are taken into account when tracking the MPPT.

$\frac{dI}{dV} = -\frac{I}{V}$ at MPPT (8)

$\frac{dI}{dV} > -\frac{I}{V}$ at the left of MPPT (9)

$\frac{dI}{dV} < -\frac{I}{V}$ at the right of MPPT (10)

### 2.3.3. Technique fractional open circuit voltage (FVOC) technique

This technique is based on the nearly linear relationship between the open circuit voltage VOC and the photovoltaic panel's optimal voltage VMPP [21]-[23]. The relationship between $V_{OC}$ and $V_{MPP}$ is given by the (11).

$V_{MPP} = k_v.V_{oc}$ (11)

where Kv the coefficient of between between 0.71 and 0.8 varies. The flowchart in Figure 9 illustrates the FVOC technique.

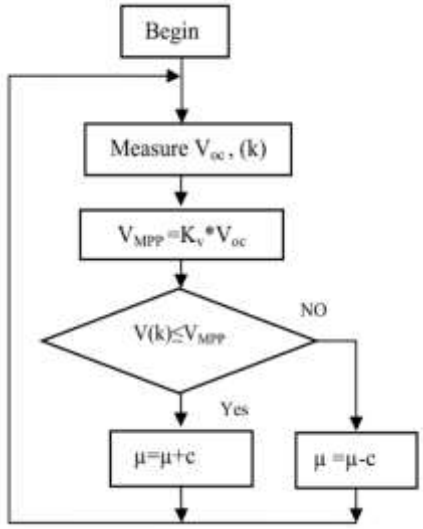


Figure 9. Flowchart of FVOC technique

### 2.3.4. Fractional short circuit current (FSCC) technique

This technique is linear in response and there is almost a direct correlation between the optimum $I_{MPP}$ and the short circuit current $I_{SC}$ change of the PV in different atmospheric conditions [24], [25]. The relation between $I_{MPP}$ and Isc is given by the (12):

$$I_{MPP} = k_c . I_{sc} \quad (12)$$

where $k_c$ is the coefficient of between 0.78 and 0.92 varies. The flowchart in Figure 10 illustrates the FSCC technique.

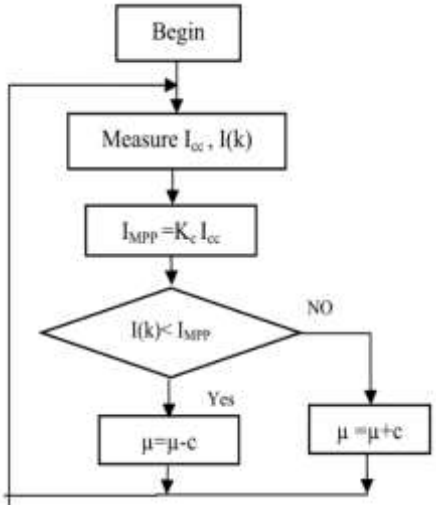


Figure 10. Flowchart of FSCC technique

## 3. RESULTS AND DISCUSSION

As illustrated in Figure 11, the considered photovoltaic system generates 20 kW and is designed, simulated, and implemented. This system is divided into six stages. The first stage is a photovoltaic array with 80 panels, the second stage is a boost converter DC/DC, and the inverter (3-level single-phase bridge, H

voltage source). The fourth stage includes a passive LCL (LPF) filter connected to the main off-grid fifth dynamic load circuit, and the final stage is a battery.

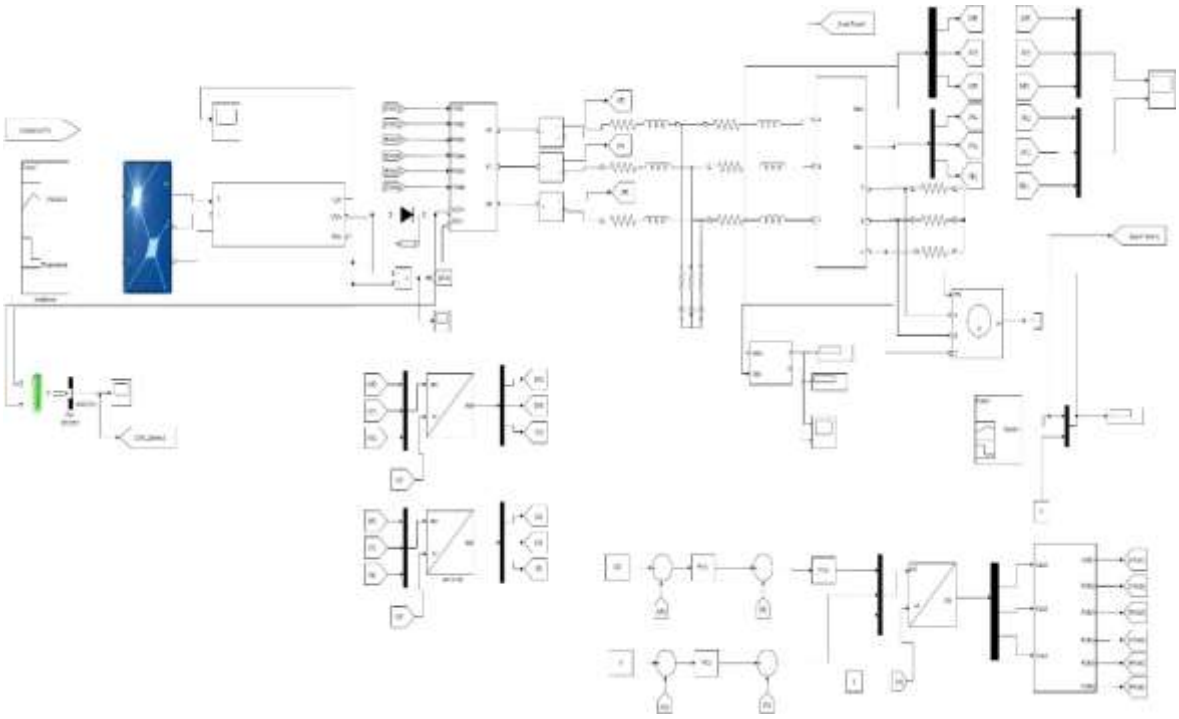

Figure 11. The simulation of PV system

Table 2 show MPPT controller at fixed temperatures (T) with range of irradiance (G), while Table 3 show MPPT controller at different temperatures (T) with fixed irradiance (G). Figures 12 (a)-(d) and Figure 13 (a)-(d)illustrate the step response of power for various MPPT techniques at different temperatures (T) 25°$C$, irradiance (G) 1000 W/$m^2$ and temperature (T) 15°$C$, irradiance (G) 600 W/$m^2$, respectively. Table 4 and Table 5 show comparison between the four MPPT techniques after take 10 (sec) of time operation temperature (T) 25°$C$, irradiance (G) 1000 W/$m^2$ and temperature (T) 15°$C$, Irradiance (G) 600 W/$m^2$, respectively, mention overshoot, undershoot, rise time and setting time.

Table 2. MPPT controller fixed (T=25), range of (G=200, 600, 1000)

| G | V-PV | P&O | | INC | | FVOC | | FSCC | |
|---|---|---|---|---|---|---|---|---|---|
| | | V | Error | V | Error | V | Error | V | Error |
| 200 | 360.798 | 360.6 | 0.198 | 359.8 | 0.998 | 352.5 | 8.298 | 351.082 | 9.716 |
| 600 | 360.806 | 360.6 | 0.209 | 359.8 | 1.009 | 352.6 | 8.209 | 351.2 | 9.609 |
| 1000 | 360.826 | 360.6 | 0.226 | 359.8 | 1.026 | 352.6 | 8.226 | 351.21 | 9.616 |

Table 3. MPPT controller range of (T=10, 30, 50), fixed (G=1000)

| G | V-PV | P&O | | INC | | FVOC | | FSCC | |
|---|---|---|---|---|---|---|---|---|---|
| | | V | Error | V | Error | V | Error | V | Error |
| 10 | 360.826 | 360.6 | 0.226 | 360.17 | 0.656 | 353.16 | 7.666 | 351.93 | 8.896 |
| 30 | 360.826 | 360.6 | 0.226 | 359.8 | 1.026 | 352.6 | 8.226 | 351.21 | 9.616 |
| 50 | 360.267 | 351.02 | 0.247 | 349.68 | 1.587 | 347.87 | 3.397 | 349.67 | 5.597 |

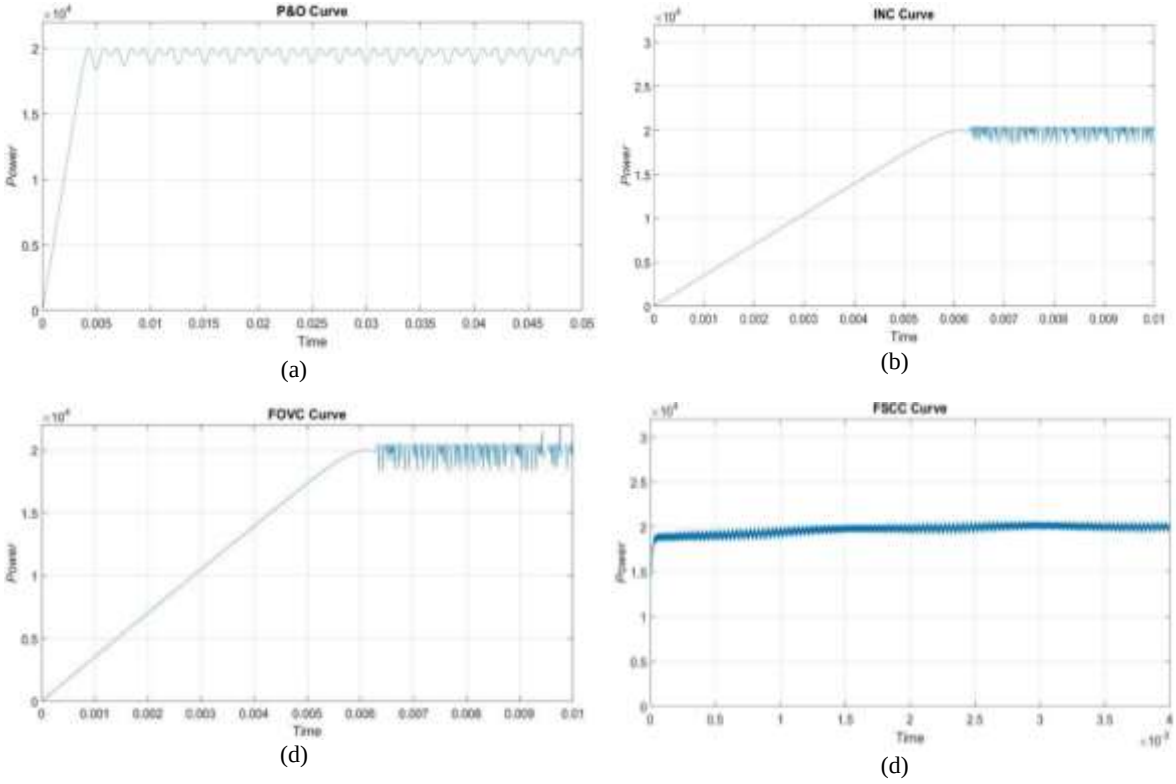


Figure 12. The result of power from different techniques in temperature (T) 25°$C$, (a) irradiance (G) 1000 W/$m^2$; (b) INC curve; (c) FOVC curve; (d) FSCC curve

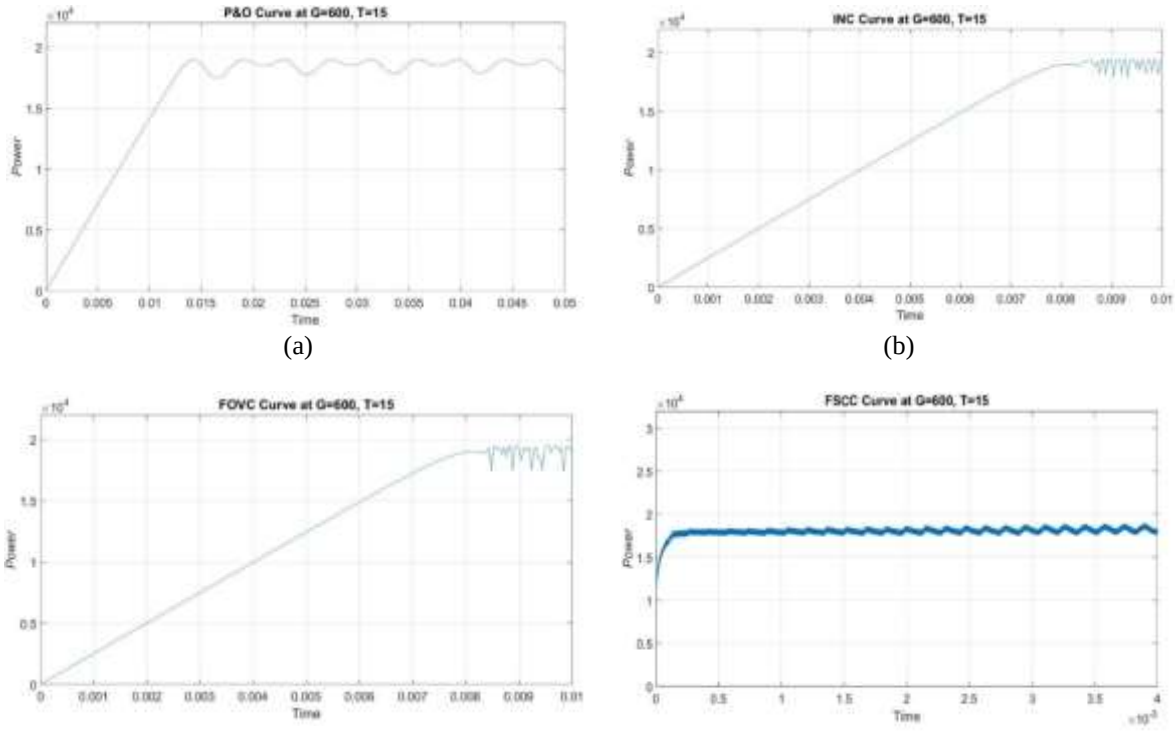


Figure 13. The result of power from different techniques in temperature (T) 15°$C$, (a) irradiance (G) 600 W/$m^2$; (b) INC curve; (c) FOVC curve; and (d) FSCC curve

Table 4. Performance comparison of MPPT techniques for PV at T= 25°$C$, G = 1000 W/$m^2$

| MPPT Techiques | Undershoot (%) | Overshoot (%) | Settling time (sec) | Rise time (sec) |
|---|---|---|---|---|
| P&O | 5.83 | 0.89 | 20.437 | 6.843 |
| INC | 1.89 | 10.75 | 18.425 | 6.954 |
| FVOC | 6.92 | 5.87 | 9.835 | 5.217 |
| FSSC | 7.38 | 5.42 | 9.672 | 5.372 |

Table 5. Performance comparison of MPPT techniques for PV at T= 15°$C$, G = 600 W/$m^2$

| MPPT Techiques | Undershoot (%) | Overshoot (%) | Settling time (sec) | Rise time (sec) |
|---|---|---|---|---|
| P&O | 4.21 | 2.57 | 21.846 | 8.492 |
| INC | 19.57 | 4.28 | 11.487 | 8.921 |
| FVOC | 14.83 | 3.37 | 16.475 | 7.647 |
| FSSC | 16.48 | 3.82 | 22.749 | 7.384 |

## 4. CONCLUSION

This study also includes the design and simulation of a 20-kW photovoltaic-powered pump that uses simple methods, such as PVP. In summary, the results can be stated is being as: The best oscillation in P&O MPPT technique; the best rise time, settling time in Fractional voltage current circuit (open, short) MPPT; At T=15°$C$, G=600 W/$m^2$ the Incremental conductance MPPT best performance in settling time.

## REFERENCES


[1] P. Soulatiantork, "Performance comparison of a two PV module experimental setup using a modified MPPT algorithm under real outdoor conditions," *Solar Energy*, vol. 169, pp. 401-410, July 2018, doi: 10.1016/j.solener.2018.04.065.

[2] A. K. Tiwari *et al*., "Effect of head and PV array configurations on solar water pumping system," in *Materials Today: Proceedings*, October 2020, doi: 10.1016/j.matpr.2020.09.200.

[3] R. Foster, and A. Cota, "Solar water pumping advances and comparative economics," *Energy Procedia*, vol. 57, pp. 1431-1436, 2014, doi: 10.1016/j.egypro.2014.10.134.

[4] E. Gupta, "The impact of solar water pumps on energy-water-food nexus: Evidence from Rajasthan, India," *Energy Policy*, vol. 129, pp. 598-609, Juni 2019, doi: 10.1016/j.enpol.2019.02.008.

[5] Y. Zhu, M. K. Kim, and H. Wen, "Simulation and analysis of perturbation and observation-based self-adaptable step size maximum power point tracking strategy with low power loss for photovoltaics," *Energies*, vol. 12, no. 1, p. 92, December 2018, doi: 10.3390/en12010092.

[6] K. S. Tey and S. Mekhilef, "Modified incremental conductance algorithm for photovoltaic system under partial shading conditions and load variation," *IEEE Transactions on Industrial Electronics*, vol. 61, no. 10, pp. 5384-5392, Oct. 2014, doi: 10.1109/TIE.2014.2304921.

[7] M. M. Shebani, T. Iqbal, and J. E. Quaicoe, "Comparing bisection numerical algorithm with fractional short circuit current and open circuit voltage methods for MPPT photovoltaic systems," in *2016 IEEE Electrical Power and Energy Conference (EPEC)*, 2016, pp. 1-5, doi: 10.1109/EPEC.2016.7771689.

[8] G. B. Ingale, S. Padhee, and U. C. Pati, "Design of stand alone PV system for DC-micro grid," in *2016 International Conference on Energy Efficient Technologies for Sustainability (ICEETS)*, 2016, pp. 775-780, doi: 10.1109/ICEETS.2016.7583852.

[9] S. Obukhov, A. Ibrahim, A. A. Zaki Diab, A. S. Al-Sumaiti, and R. Aboelsaud, "Optimal performance of dynamic particle swarm optimization based maximum power trackers for stand-alone PV system under partial shading conditions," *IEEE Access*, vol. 8, pp. 20770-20785, 2020, doi: 10.1109/ACCESS.2020.2966430.

[10] Z. M. Ali, N. V. Quynh, S. Dadfar, and H. Nakamura, "Variable step size perturb and observe MPPT controller by applying θ-modified krill herd algorithm-sliding mode controller under partially shaded conditions," *Journal of Cleaner Production*, vol. 271, p. 122243, October 2020, doi: 10.1016/j.jclepro.2020.122243.

[11] M. A. Hasan, and S. K. Parida, "An overview of solar photovoltaic panel modeling based on analytical and experimental viewpoint," *Renewable and Sustainable Energy Reviews*, vol. 60, pp. 75-83, July 2016, doi: 10.1016/j.rser.2016.01.087.

[12] K. J. Singh, K. L. R. Kho, S. J. Singh, Y. C. Devi, N. B. Singh, and S. K. Sarkar, "Artificial neural network approach for more accurate solar cell electrical circuit model," *International Journal on Computational Science & Applications*, vol. 4, pp. 101-116, 2014, doi: 10.5121/IJCSA.2014.4310.

[13] Canadian Solar, "Datasheet: CS6P-250M," 2012. [Online]. Available: https://selasenergy.gr/technical%20data/solar-panels/Canadian%20Solar/CS6P/CS6P-255M%20mono.pdf.

[14] H. A. Attia, and F. delAma Gonzalo, "Stand-alone PV system with MPPT function based on fuzzy logic control for remote building applications," *International Journal of Power Electronics and Drive System (IJPEDS)*, vol. 10, no. 2, pp. 842-851, June 2019, doi: 10.11591/ijpeds.v10.i2.pp842-851.

[15] M. A. Islam, A. Merabet, R. Beguenane, H. Ibrahim, and H. Ahmed, "Simulation based study of maximum power point tracking and frequency regulation for stand-alone solar photovoltaic systems," in *International Conference on Renewable Energies and Power Quality (ICREPQ'14)*, vol. 1, no. 12, April 2014, pp. 1-6, doi:

10.24084/repqj12.378.
[16] Z. Massaq, A. Abounada, and R. Mohamed, "Robust non-linear control of a hybrid water pumping system based on induction motor," *International Journal of Power Electronics and Drive System (IJPEDS)*, vol. 11, no. 4, pp. 1995-2006, December 2020, doi: 10.11591/ijpeds.v11.i4.pp1995-2006.
[17] A. A. Abdulrazzaq, and A. H. Ali, "Efficiency performances of Two MPPT algorithms for PV system with different solar panels irradiances," *International Journal of Power Electronics and Drive System (IJPEDS)*, vol. 9, no. 4, pp. 1755-1764, December 2018, doi: 10.11591/ijpeds.v9.i4.pp1755-1764.
[18] M. W. Rahman, C. Bathina, V. Karthikeyan, and R. Prasanth, "Comparative analysis of developed incremental conductance (IC) and perturb & observe (P&O) MPPT algorithm for photovoltaic applications," in *2016 10th International Conference on Intelligent Systems and Control (ISCO)*, 2016, pp. 1-6, doi: 10.1109/ISCO.2016.7726991.
[19] M. Naidji, M. Boudour, and F. Achouri, "Modeling and control of photovoltaic systems integrated to distribution networks," in *2018 International Conference on Electrical Sciences and Technologies in Maghreb (CISTEM)*, 2018, pp. 1-6, doi: 10.1109/CISTEM.2018.8613324.
[20] M. A. Elgendy, D. J. Atkinson, and B. Zahawi, "Experimental investigation of the incremental conductance maximum power point tracking algorithm at high perturbation rates," *IET Renewable Power Generation*, vol. 10, no. 2, pp. 133-139, September 2015, doi: 10.1049/iet-rpg.2015.0132.
[21] H. Abid, F. Tadeo, A. Toumi, and M. Chaabane, "MPPT of a photovoltaic panel based on Takagi-Sugeno and fractional algorithms," *International Review of Automatic Control*, vol. 7, no. 3, pp. 245-253, May 2014.
[22] K. R. Bharath and E. Suresh, "Design and implementation of improved fractional open circuit voltage based maximum power point tracking algorithm for photovoltaic applications," *International Journal of Renewable Energy Research (IJRER)*, vol. 7, no. 3, pp. 1108-1113, 2017.
[23] S. Baroi, P. C. Sarker, and S. Baroi, "An improved MPPT technique-alternative to fractional open circuit voltage method," in *2017 2nd International Conference on Electrical & Electronic Engineering (ICEEE)*, 2017, pp. 1-4, doi: 10.1109/CEEE.2017.8412909.
[24] H. A. Sher, A. F. Murtaza, A. Noman, K. E. Addoweesh, K. Al-Haddad, and M. Chiaberge, "A new sensorless hybrid MPPT algorithm based on fractional short-circuit current measurement and P&O MPPT," *IEEE Transactions on Sustainable Energy*, vol. 6, no. 4, pp. 1426-1434, Oct. 2015, doi: 10.1109/TSTE.2015.2438781.
[25] H. A. Sher, A. F. Murtaza, A. Noman, K. E. Addoweesh, and M. Chiaberge, "An intelligent control strategy of fractional short circuit current maximum power point tracking technique for photovoltaic applications," *Journal of Renewable And Sustainable Energy*, vol. 7, no. 1, p. 13114, January 2015, doi: 10.1063/1.4906982.